Low frequency noise from MW wind turbines

Mechanisms of generation and its modeling

Aagaard Madsen , Helge

Publication date:
2008

Document Version
Publisher's PDF, also known as Version of record

Risø-R-Report

Low frequency noise from MW wind turbines -- mechanisms of generation and its modeling

Helge Aagaard Madsen

Risø-R-1637(EN)

Risø National Laboratory
Technical University of Denmark
Roskilde, Denmark
April 2008

Author: Helge Aagaard Madsen
Title: Low frequency noise from MW wind turbines -- mechanisms of generation and its modeling
Department: Department of Wind Energy

Risø-R-1637(EN)
April 2008

Abstract (max. 2000 char.):

During the present project the mechanisms of generation of low frequency noise (LFN) for upwind rotors has been investigated. A 3.6 MW turbine has been simulated with a noise prediction model from NASA in US. Running the model on this turbine a number of important turbine design parameters with influence on the LFN have been identified as well as other parameters not linked to the turbine design. Of important parameters can be mentioned

- rotor rotational speed
- blade/tower clearance
- rotor configuration - upwind/downwind
- unsteadiness/turbulence in inflow

Further, the directivity characteristics of LFN has been computed as well as reduction in noise as function of distance from the turbine.
In general low levels of LFN has been computed for the upwind rotor in standard configuration.

ISSN 0106-2840
ISBN 978-87-550-3660-4

Contract no.:
Ens. Journalnr. 033001/33032-0081

Group's own reg. no.:
1125010-01

Sponsorship:
The Danish Energy research programme EFP-2006

Cover :

Pages: 36
Tables: 2
References: 8

Information Service Department
Risø National Laboratory
Technical University of Denmark
P.O.Box 49
DK-4000 Roskilde
Denmark
Telephone +45 46774004
bibl@risoe.dk
Fax +45 46774013
www.risoe.dk

Contents

Preface

This report describes the work and the results achieved by Risoe DTU during its participation in the EFP-2006 project ”Lavfrekvent støj fra store vindmøller– kvantificering af støjen og vurdering af genevirkningen” “

Summary

A considerable research on low frequency noise from wind turbine rotors was performed in the period from the late seventies to the mid nineties in particular in US and to some extent in Sweden. The reason was that in these two countries a number of MW turbine with a downwind rotor was build in this period and in some cases the low frequency noise (LFN) caused annoyance of people living in the neighborhood of the turbines. The research led to the development of a code for prediction of LFN and this code has been implemented at Risoe DTU.

In previous studies at Risoe DTU the LFN for downwind rotors has been investigated using this model. It was found that the unsteadiness of the flow behind the tower contributed significantly to the total LFN sound pressure level (SPL) with as much as 20 dB.

During the present project the causes of LFN for upwind rotors has been investigated. A 3.6 MW turbine has been modeled with the above mentioned noise prediction model. Running the model on this turbine a number of important turbine design parameters with influence on the LFN have been identified as well as other parameters not linked to the turbine design. Of important parameters can be mentioned

- rotor rotational speed
- blade/tower clearance
- rotor configuration - upwind/downwind
- unsteadiness/turbulence inflow

Further the directivity characteristics of LFN has been computed as well as reduction in noise as function of distance from the turbine.

In general low levels of LFN has been computed for the upwind rotor in standard configuration.

1 Introduction

At the beginning of the development of the modern wind turbines in the late seventies different rotor concepts were considered and investigated. Among them was the two-bladed teetered downwind rotor which has both advantages and drawbacks compared with the three-bladed upwind rotor. One of the main advantages of the downwind two-bladed rotor is that the use of a teetering hinge can effectively reduce the bending moments transferred to the shaft when compared with a rotor with a stiff hub. Finally, a free yawing or high flexible yawing rotor concept is easier to obtain on a downwind rotor due to the restoring yaw moment from the rotor thrust.

However, a major drawback of the downwind rotor is a considerable generation of low frequency (thumping) noise typically in the range from 20 to 100 Hz which can cause annoyance of nearby residents. Low frequency noise was experienced on the MOD-1 2 MW turbine[1] and other downwind turbines in US[2] as well as on the 3 MW Maglarp turbine[3] in Sweden. On all turbines the noise generation was linked to the blade passing the wake behind the tower, Figure 1, which for the Swedish turbine was a tubular tower, whereas the MOD-1 turbine had a lattice tower with four main poles.

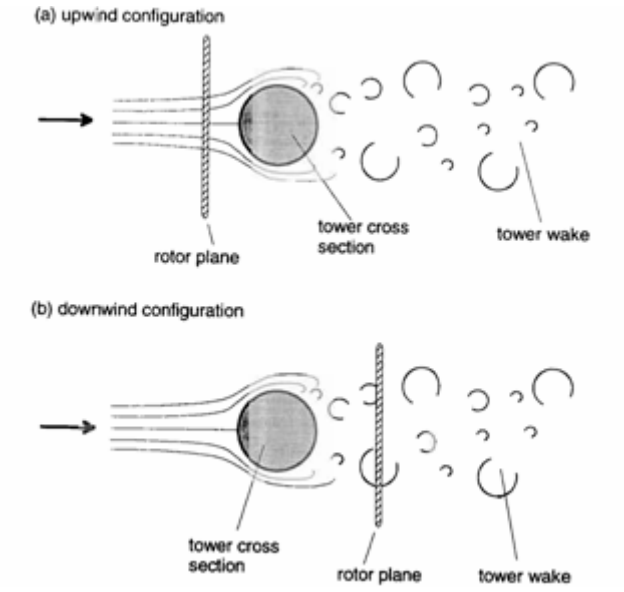

Figure 1 The disturbed flow behind the tower results in highly unsteady aerodynamic blade forces which in the final end is the main cause of low frequency noise (illustration from Wagner[4]).

A summary of the low frequency noise results from 8 different turbines in US were presented by Sheperd and Hubbard[5]. They present measured SPL for two two-bladed turbines with a downwind rotor, Figure 2, and it can be seen that there is a considerable low frequency noise which they ascribe to the bladed passing through the velocity deficit behind the tower.

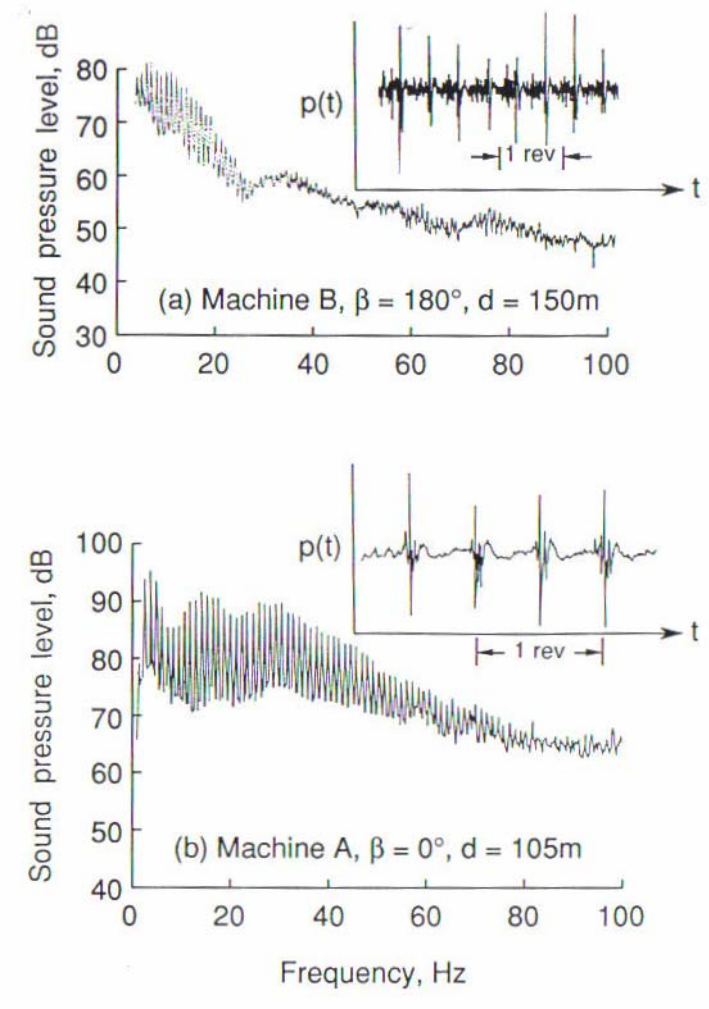

Figure 2 Measured sound pressure level (SPL) in the vicinity of two turbines with a down wind two-bladed rotor. Machine B has a 79.2 m rotor and a twelve sided tower of shell construction. Machine A has a two-bladed 61m diameter downwind rotor and a four-legged open truss tower. Direction β=180 deg. is downwind and β=0 deg. is upwind. d denotes the distance from the turbine. Noise due to blade passage of the disturbed flow behind the tower. Figure from Shepherd and Hubberd [5].

Sheperd and Hubbard[5] also present measurements of low frequency noise from two turbines with an upstream rotor and with a diameter of 43 m and 95 m, respectively. The SPL level for the two turbines is considerably lower than for the two turbines with downwind rotors. The noise that is generated is described by Sheperd and Hubbard to be caused by irregularities in the inflow to the turbines such as terrain effects.

The research in US on low frequency noise from wind turbines performed in the period from the late seventies to the mid nineties led to the development of a model for computation of low frequency noise, the NASA-LeRC wind turbine sound prediction code by A. Viterna[6]. This code was implemented at Risoe DTU a few years ago and before the initiation of the present project. During this previous work the focus has been on noise generation from turbines with two-bladed, down-wind rotors. One of the main objectives of these previous studies has been to clarify and quantify the importance of the unsteadiness of the flow behind the tower such as vortex shedding. The results have

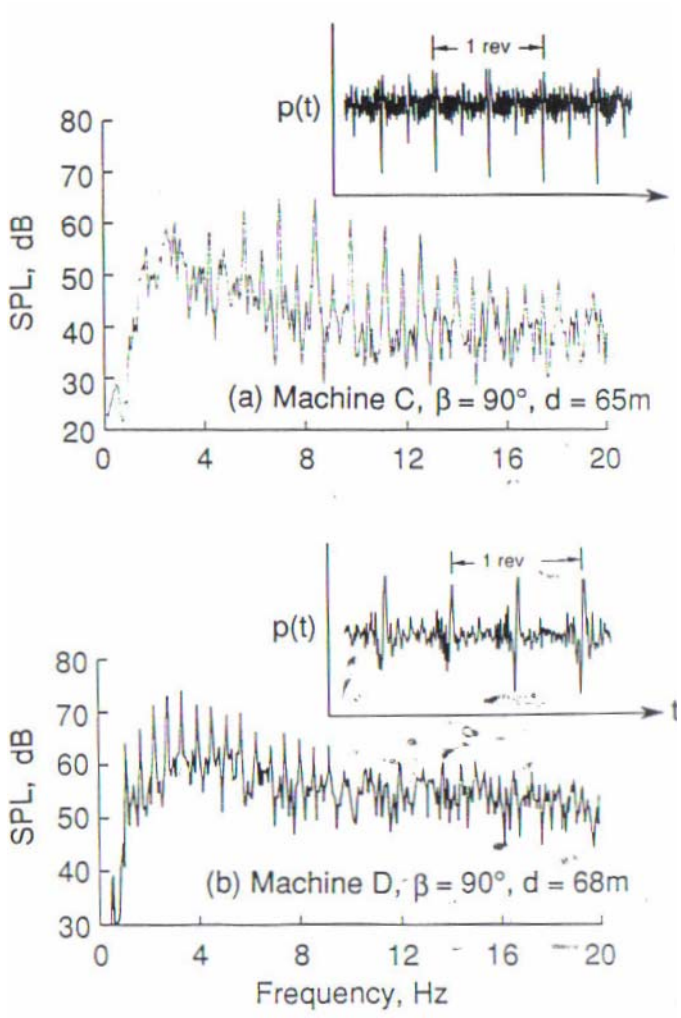

Figure 3 Measured sound pressure level (SPL) in the vicinity of two turbines with a an upwind, two-bladed rotor. Machine C has a two-bladed 43.3m diameter rotor and machine D has a two-bladed 97.5 m rotor. Note that the listener direction is in the rotor plane 65 m and 68 m from the turbine. The cause of the noise is thought to be distortion of the inflow to the turbines from terrain irregularities upstream. Figure from Shepherd and Hubberd[5].

shown that the unsteadiness can add additional 10 dB to the noise based on a steady deficit and in some cases with coincidence of the blade passing frequency with vortex shedding frequency the increase can be up to 20 dB. These results are contained in a paper[7] which was presented in January 2007 at the AIAA conference in Reno. The paper is enclosed as Appendix B in the present report.

1.1 Contents and structure of the present report

The focus in the present project has been on noise generation from MW turbines with an upstream rotor. The low frequency noise (LFN) model is first briefly described and then follows a number of results which are aimed at clarifying what are the major design parameters and other parameters influencing the low frequency noise at a listener position nearby the turbine.

2 Description of numerical model

2.1 The acoustic model

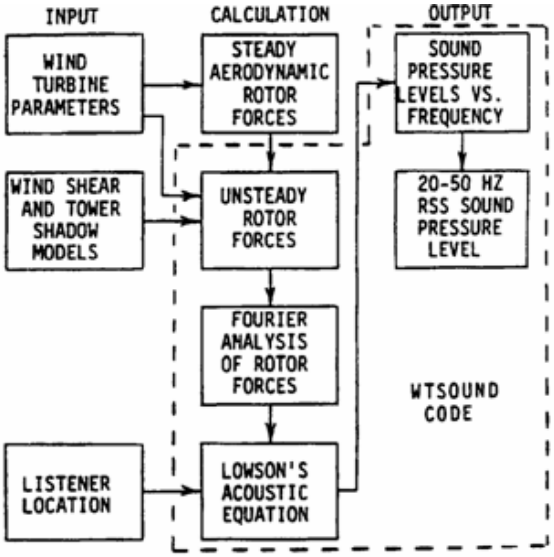

Figure 4 The original flow chart of Viterna showing the main components and steps in computation of low frequency noise. (from Viterna[6]).

The model is based on established theories and methods for computation of propeller and compressor noise. In a compressor there is stationary blade rows and behind them follows rotating blades which are passing through the velocity deficits and disturbances of the stationary blades. Lowson[8] has developed a general theory for such cases relating the sound pressure level (SPL) to the Fourier coefficients for the unsteady aerodynamic forces on the blades.

A number of assumption and simplifications have been made in the theory of Lowson in order to end up with a relatively compact model. One of the assumptions is to concentrate the unsteady aerodynamic forces on the blades at one radial station. However, for observation points not too close to the turbine this seems to be reasonable.

To compute the unsteady aerodynamic forces the general aeroelastic code HAWC2 developed at Riso DTU is used. The HAWC2 code has different sub-models to handle the computation of the unsteady blade aerodynamics such as the Beddoes Leishman model for unsteady blade aerodynamics.

The implementation of the model for computation follows the description by Viterna[6].

The RMS pressure variation of the n[th] harmonic of the blade passage frequency is given by the following equations:

$$P_n = \frac{k_n\sqrt{2}}{4\pi s}\Big\{ \sum_{p=1}^{\infty} \left[\begin{array}{l} e^{-im(\Phi-\pi/2)}\, J_{nB-p}\left(k_n r_m \sin\gamma\right)\cdot\left(a_p^F \cos\gamma - \dfrac{nB-p}{k_n r_m} a_p^Q \right) + \\ \\ e^{im(\Phi-\pi/2)}\, J_{nB+p}\left(k_n r_m \sin\gamma\right)\cdot\left(a_{-p}^F \cos\gamma - \dfrac{nB+p}{k_n r_m} a_{-p}^Q \right) \end{array} \right]$$

$$J_{nB}\left(k_n\, r_m \sin(\gamma)\right)\left(F^s \cos(\gamma) - \frac{n\,B}{k_n\, r_m} Q^s \right) \Big\} \qquad (1)$$

where $k_n = \dfrac{nB\Omega}{c_0}$ (2)

a_p^F , a_p^Q	are Fourier coefficients of rotor thrust and torque, respectively.
B	number of blades
s	distance to rotor in [m]
γ, Φ	azimuth and altitude angle, respectively, as taken from the point of observation to the rotor center, cf. Figure 5
r_m	radius on blade, where thrust and torque is supposed to be concentrated
J	standard Bessel function
c_0	speed of sound
F^s, Q^s	steady thrust and steady torque, respectively.

The Fourier coefficients of rotor thrust a_p^T and rotor torque a_p^Q are defined as:

$$a_p^T = \frac{1}{T}\int_0^T F(\tau) e^{ip\frac{2\pi}{T}\tau}\, d\tau \qquad (3)$$

and

$$a_p^Q = \frac{1}{T}\int_0^T Q(\tau) e^{ip\frac{2\pi}{T}\tau}\, d\tau \qquad (4)$$

where F and Q is rotor thrust and torque, respectively, and T is the time for one rotor rev. In Appendix I different methods for computation of the Fourier coefficients are compared.

Finally, the sound pressure level SPL_n for each harmonic is computed as:

$$SPL_n = 10\log_{10}\left(\frac{P_n^2}{P_{ref}^2}\right) where \qquad P_{ref} = 2\cdot 10^{-5}\ \text{Pa}. \tag{5}$$

The total sound pressure level SPL is computed by summing up the SPL_n from each harmonic:

$$SPL = 10\log_{10}\left(\frac{1}{\hat{p}_{ref}^2}\sum_n \hat{p}_n^2\right) \tag{6}$$

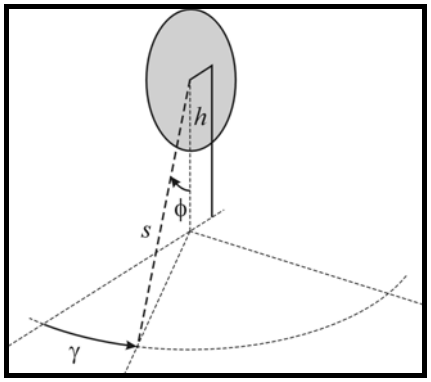

Figure 5. Definition of azimuth and altitude angles used in the acoustic model.

3 Simulations results

3.1 Model data for Siemens 3.6MW turbine

Computations were performed on the Siemens 3.6 MW turbine, which has been tested at the Høvsøre test field for MW turbines. Measurements of low frequency noise from this turbine have been performed by DELTA within the present project and a comparison with measured noise will be presented later.

Data on the turbine necessary to run the computations were received from Siemens. The turbine is an upwind turbine, pitch controlled and with variable speed. The coning of the rotor is 3.5 deg. and the tilt is 6 deg. Together with a shaft length of 3.8 m this results in a distance of around 13 m from the tower center to the blade tip, when it is passing the tower. The tower diameter is around 2.1 m at the height where the blade tip is passing the tower and this gives then a clearance of about 10.9 m. The maximum average deflection of the blade is at 11-12 m/s is around 3.5 m but with a maximum up to slightly above 5 m. This gives then a minimum clearance of 6 m.

In the simulations the turbine structure is assumed stiff. This was done because a full set of data necessary for modeling the flexibility of the turbine was not available. However, it is thought not to be a major problem as the most important parameter for the low frequency noise is the blade tip clearance to the tower and data for the deflection of the blade was received from Siemens and could be accounted for as shown below.

3.2 Noise as function of wind speed

Noise was computed at 6, 8, 10 and 12 m/s. The following turbine data were used:

Table 1 Input data used for computation of noise at different wind speed

Wind speed	pitch angle [deg.]	rotor speed [rad/s]	equivalent cone angle for blade deflection [deg.]
6	0.02	0.90	-1.7
8	-0.08	1.24	-2.8
10	-1.86	1.39	-3.5
12	1.38	1.40	-3.3

The equivalent cone angle was derived as the change in cone angle that gave the same deflection of the tip as was computed by Siemens on a flexible turbine. This was done in order to get almost the same tip clearance in the present simulations on a stiff turbine as computed on a flexible turbine.

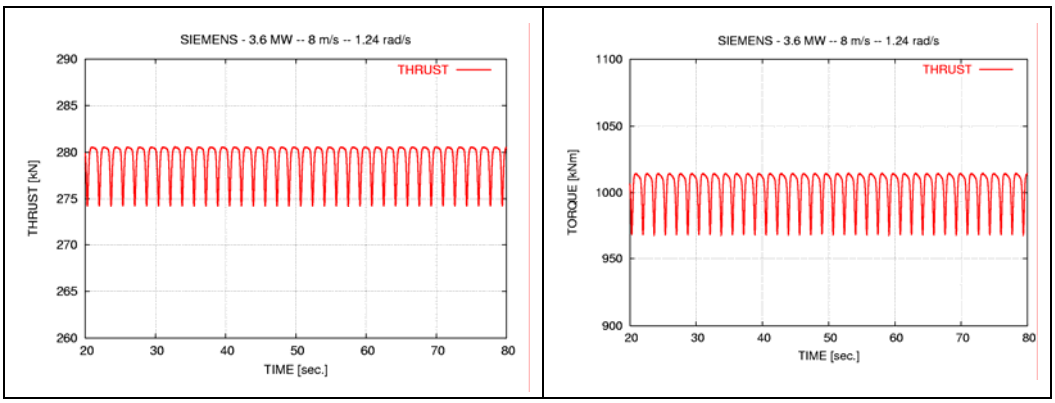

Figure 6 *Computed thrust and torque at 8 m/s.*

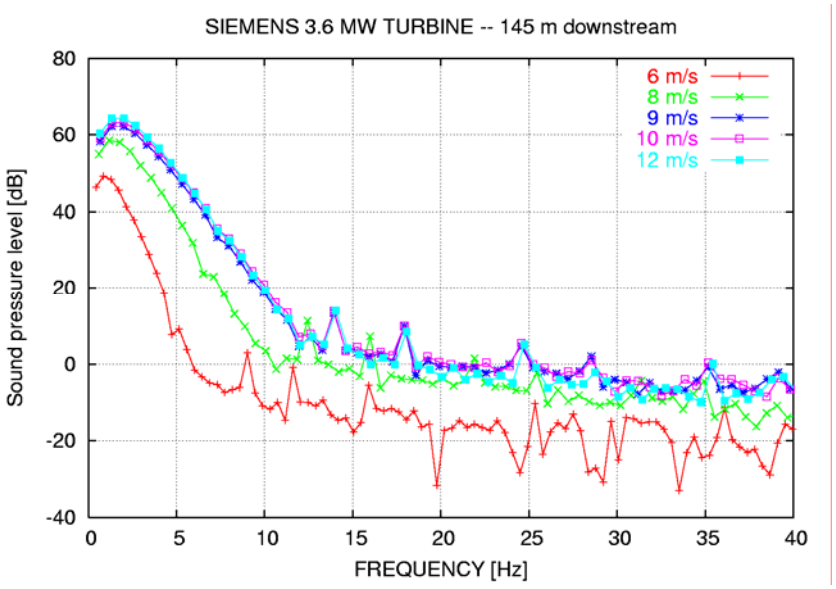

Figure 7 *Computed SLP for different wind speeds at a position of 145 m downstream the rotor.*

The computed thrust and torque at 8 m/s is shown in Figure 6. The variation in both signals occurs three times on each rev. and is due to the blade passing the tower as well as the influence of the tilt of the rotor.

For the wind speeds of 6, 8, 10 and 12 m/s the sound pressure level (SPL) at a distance of 145 m downstream the rotor and on the ground level, is shown in Figure 7. It is seen that the up to a wind speed of 9 m/s the SPL increases as function of wind speed. The main parameter causing this is that the rotational speed increases as function of wind speed but becomes constant from a wind speed around 9 m/s. It should also be noted that the main SPL level is seen for frequencies below 10-15 Hz where the hearing threshold is high of the order of 90 - 100 dB.

3.3 Noise as function of rotor/tower distance

The influence of reducing the rotor/tower distance was investigated by reducing the length of the shaft in the turbine model used for computation of the unsteady blade forces. The normal clearance at 10 m/s is around 7.5 m and this distance was reduced with 2m, 4m, 5m and 6 m, respectively. The corresponding SPL curves are shown in Figure 8 and it is seen that the rotor/tower clearance is very important for the SPL level.

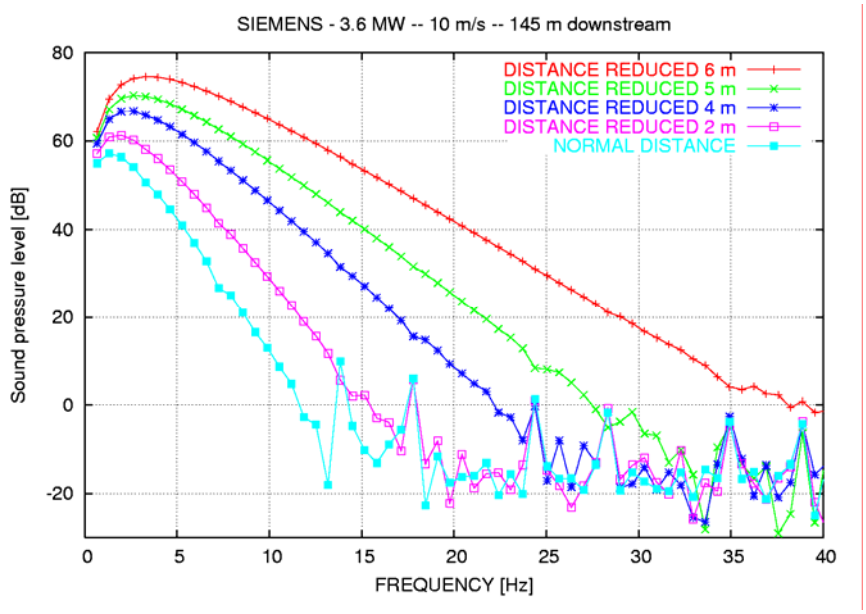

Figure 8 SPL computed for different reductions of the normal distance between tower and blade.

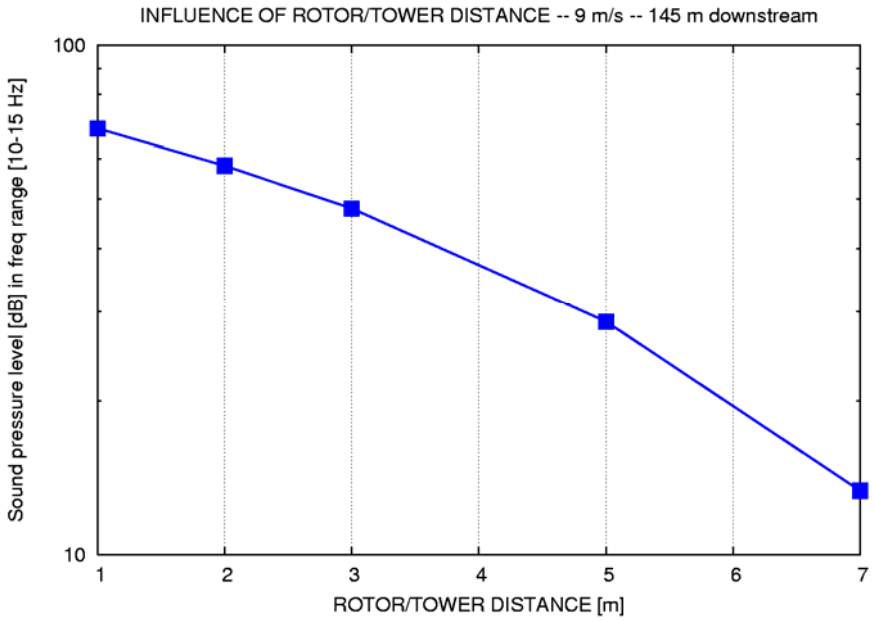

Figure 9 SPL integrated in the frequency range from 10-15 Hz and shown as function of different reductions of the normal distance between tower and blade.

3.4 Noise as function of rotor rotational speed

The next turbine design parameter that is investigated is the rotational speed. At a wind speed of 10 m/s the rotational speed was increased with 25% and reduced 25%, respectively. The corresponding SPL curves are shown in Figure 10 and a change of 25% in rotational speed gives a change in SPL of about 14 dB illustrating that this design parameter also is very important for the SPL level.

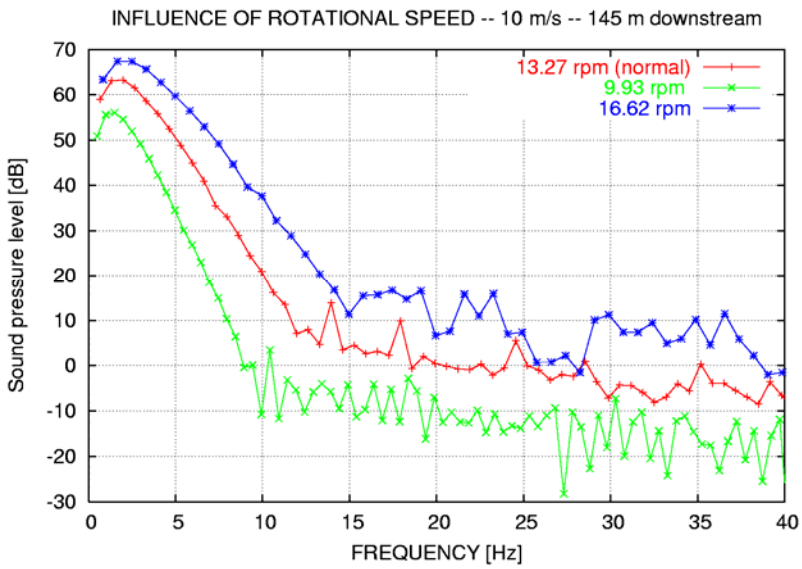

Figure 10 Computed SPL curves for a 25% increase/decrease in rotational speed and compared with normal operation.

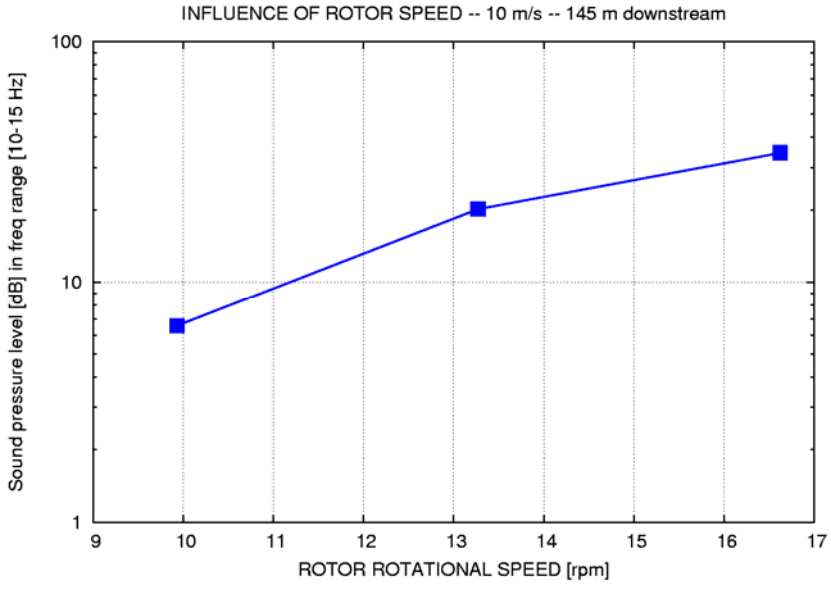

Figure 11 SPL integrated in the frequency range from 10-15 Hz shown as function of rotational speed.

3.5 Noise – rotor upstream/downstream

The importance of the two different rotor concepts, rotor upstream/downstream the tower, is illustrated below. In the present case the velocity deficit downstream the tower is assumed steady but even in this case the SPL level for a downwind rotor is higher than for an upwind rotor where the blade/tower clearance has been reduced to 1.5 m.

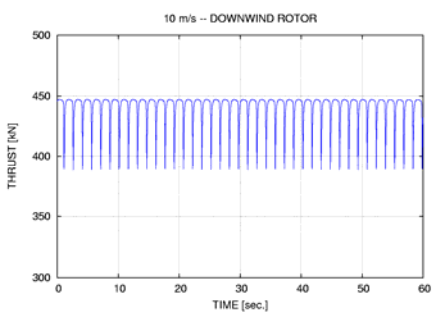

Figure 12 Time trace of thrust for a down wind rotor.

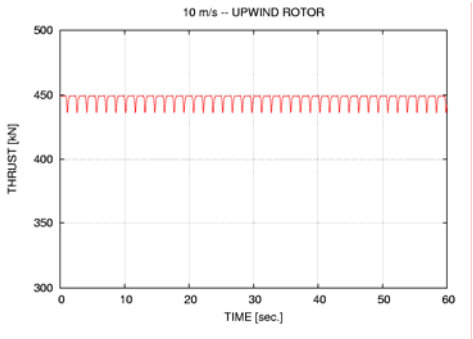

Figure 13 Time trace of thrust for an upwind rotor.

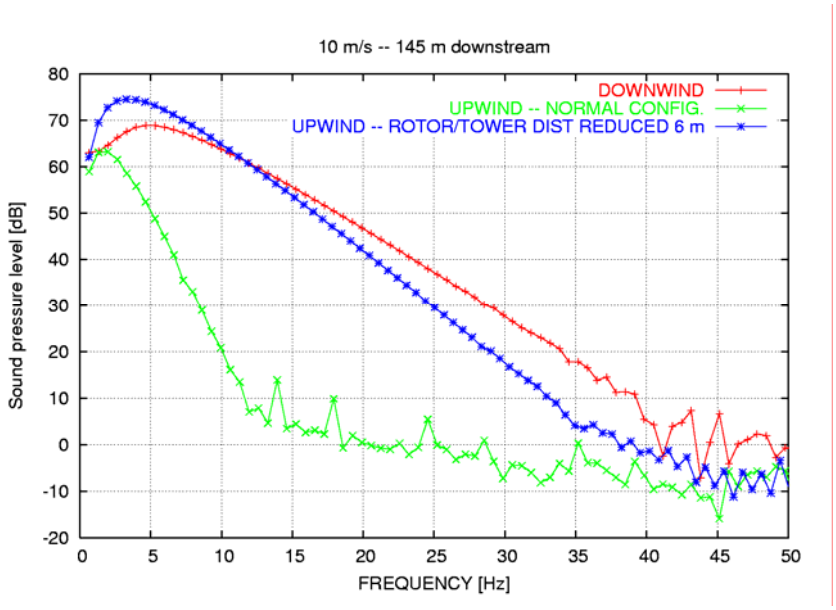

Figure 14 A comparison of the SPL for an upwind and a downwind rotor. Further, a comparison is made with an upwind rotor with the blade very close to the tower (about 1.5 m).

3.6 Influence of distance to listener

The LFN model has next been used to investigate the reduction of SPL as function of distance to the listener. SPL curves have been computed for distances 100 m. 200 m, 400 m and 800 m as shown in Figure 15 and in Table 2 the results are summarized. It is seen that the reduction in noise is 6 dB for a doubling of distance which is the theoretical result for spherical spreading. However, Shepherd and Hubbard report in their paper[5] that a reduction of only 3 dB often is measured downstream a rotor due to atmospheric defraction.

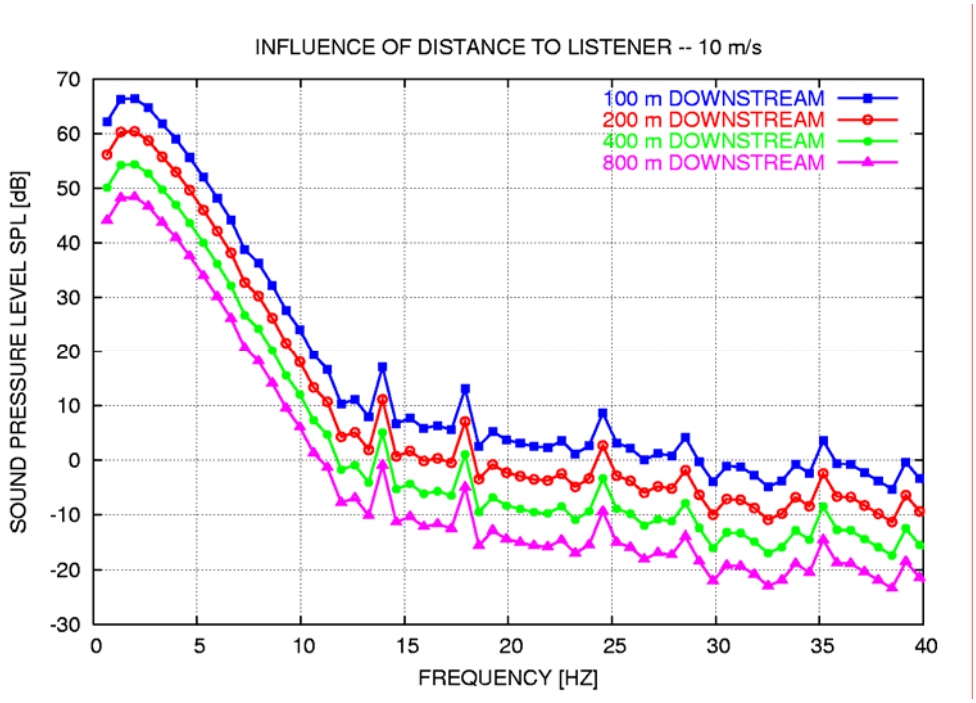

Figure 15 *Computed SPL for different distances to listener.*

Table 2 *Reduction in SPL as function of distance to listener*

Downstream distance to listener [m]	SPL [dB] in freq. range 10-15 Hz	Δ SPL [dB]
100	**23.4**	**6.0**
200	**17.4**	**6.0**
400	**11.4**	**6.0**
800	**5.4**	**6.0**

3.7 Directivity – 10 m/s

The directivity can be computed with the LFN model and for the 10 m/s case the results are shown in Figure 16 and Figure 17. It is seen that for directions deviating more that about 60 deg. from downstream direction there is a considerable reduction in SPL level, which can be up to 25 dB

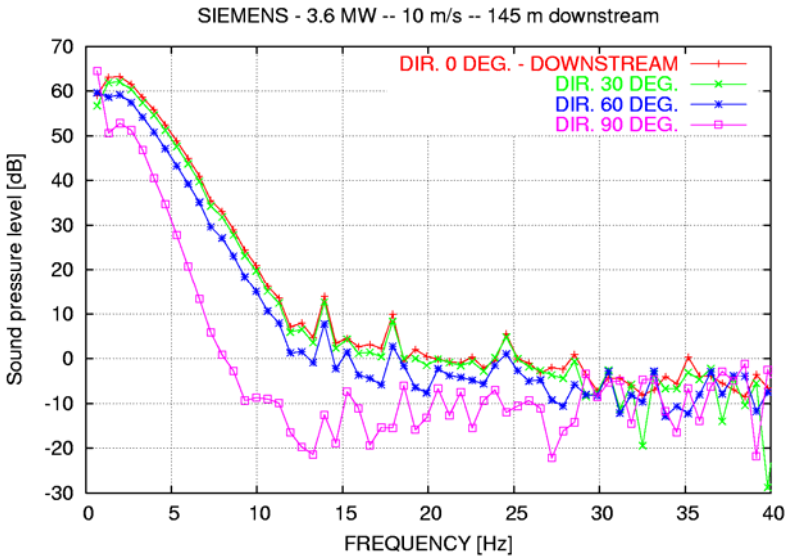

Figure 16 *Computed SPL for different angular directions to the listener.*

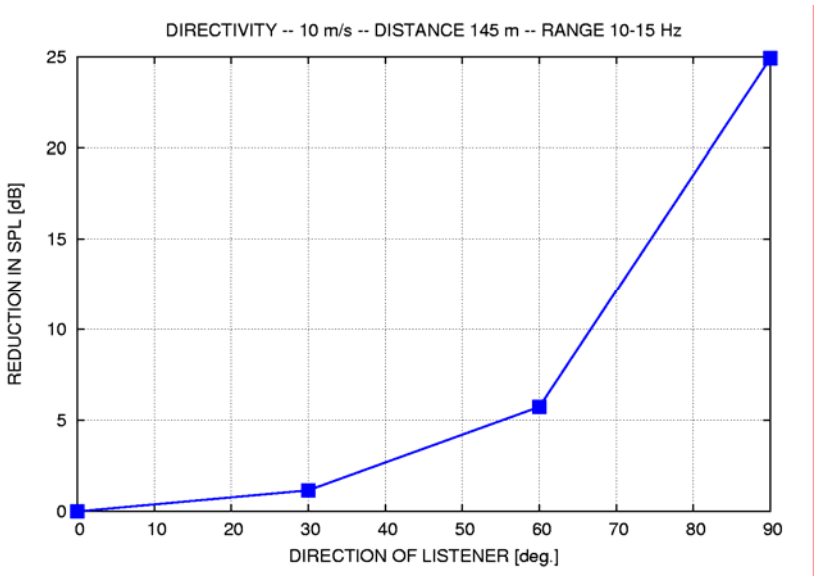

Figure 17 *Reduction in SPL as function of angular direction to listener integrated in the frequency range from 10-15 Hz.*

3.8 Comparison with measurements

For the 8 m/s case the simulations were compared with measurements performed by DELTA in the vicinity of the Siemens 3.6 MW turbine at Høvsøre. Comparing directly with the data computed so far (without influence of atmospheric turbulence) there is a big discrepancy between the measured SPL level and the computed level, Figure 18. It should however be noted that the measured values are not corrected for background noise and this could explain some of the discrepancy. Another cause for

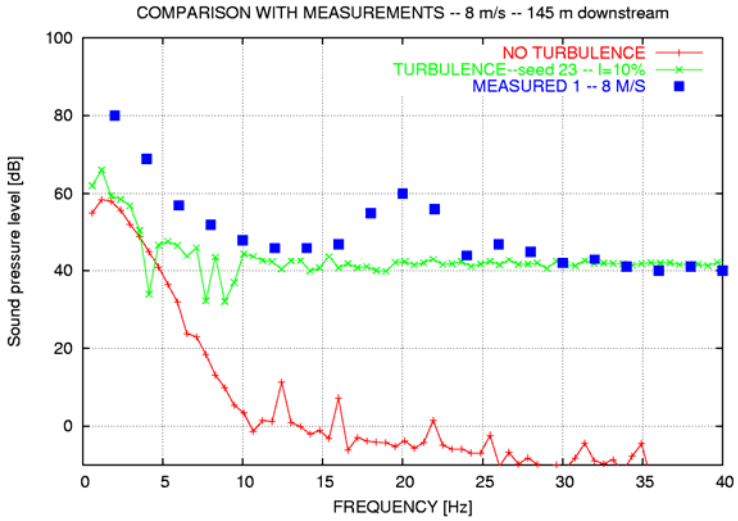

Figure 18 Comparison of measured and computed SPL levels.

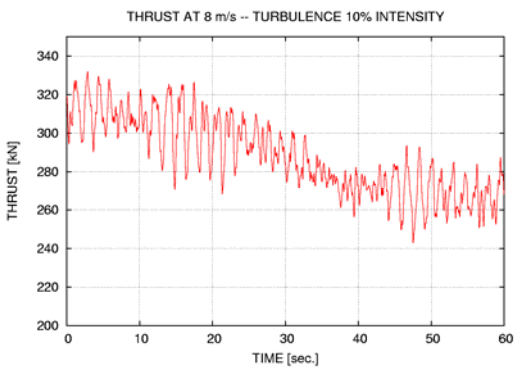

Figure 19 Time trace of computed thrust with 10 % turbulence.

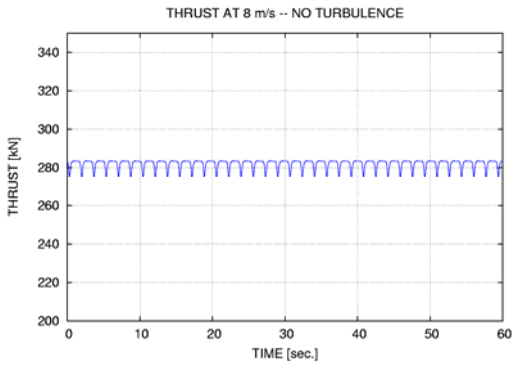

Figure 20 Time trace of computed thrust with no turbulence.

the deviations is that what is normally denoted as broadband noise (here mainly noise from turbulent inflow) adds to the levels also at these low frequencies. In the validation of the model performed by Viterna6 the measurements are corrected for contents of broadband noise. However, in the present case it was instead tried to run the aerodynamic simulations with turbulence in the inflow. When in-flow turbulence is included (in the present case 10% turbulence intensity) there is a good agreement

between measured and predicted values. The bump around 20 Hz could be a discrete frequency from the drive-train. Below 10 Hz the background noise dominates the measurements as can be seen from the measurement reports of the individual measurement campaigns.

It seems thus that in the present case the blade/tower interaction only contributes to the LFN level for frequencies below 10-15Hz and for higher frequencies it is more the interaction of the blade with the non-uniformities in the inflow such as turbulence that generates the low frequency noise.

Finally, the influence of turbulence on the time trace of thrust is shown in Figure 19 and this can be compared with the uniform inflow case in Figure 20.

4 Appendix 1

4.1 Test of Fourier transformation

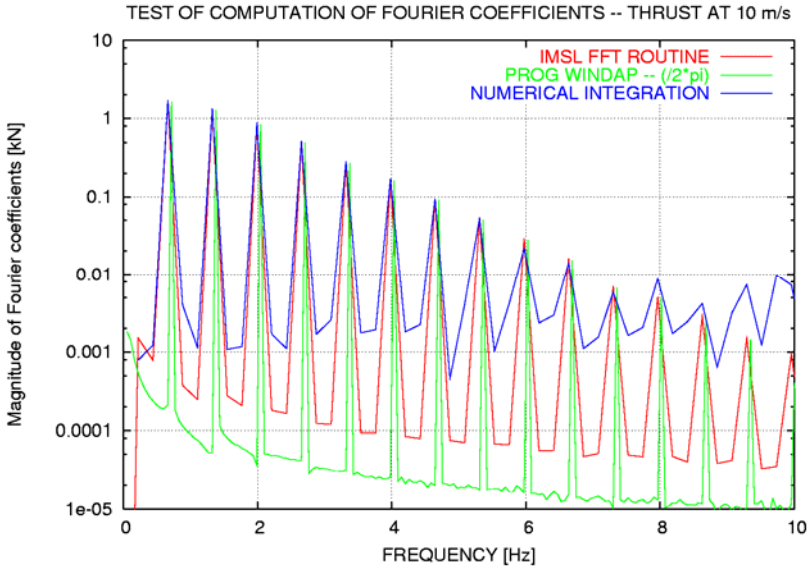

Figure 21 Fourier coefficients computed with different models. The one used in all the SPL computations is the IMSL FFT routine.

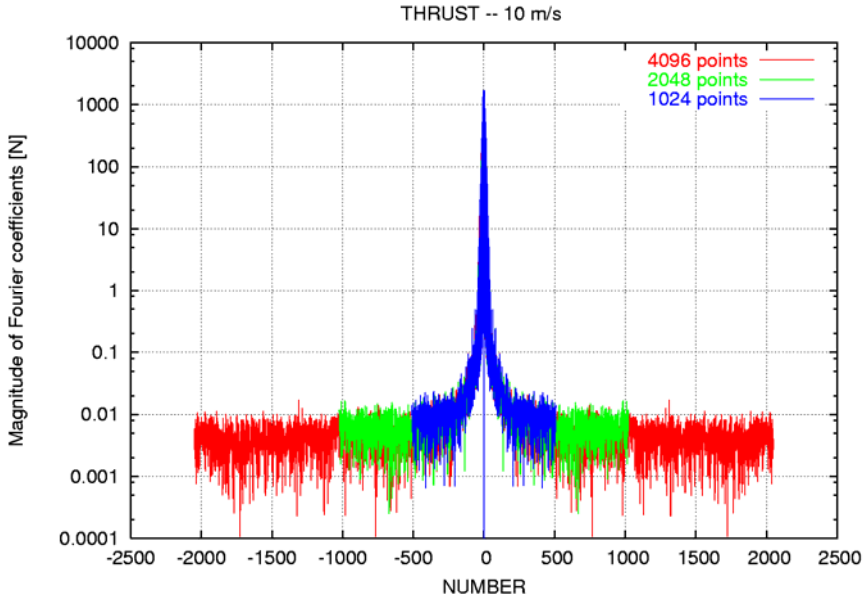

Figure 22 A test was performed of the influence of time resolution. In most cases 1024 points for 1 rev have been used.

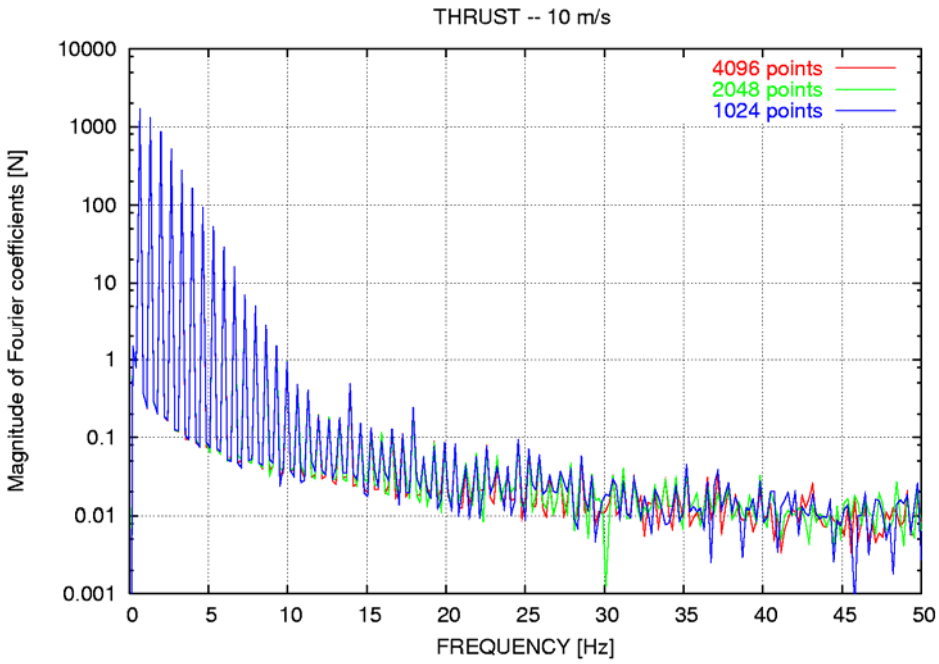

Figure 23 *Further test of the influence of time resolution.*

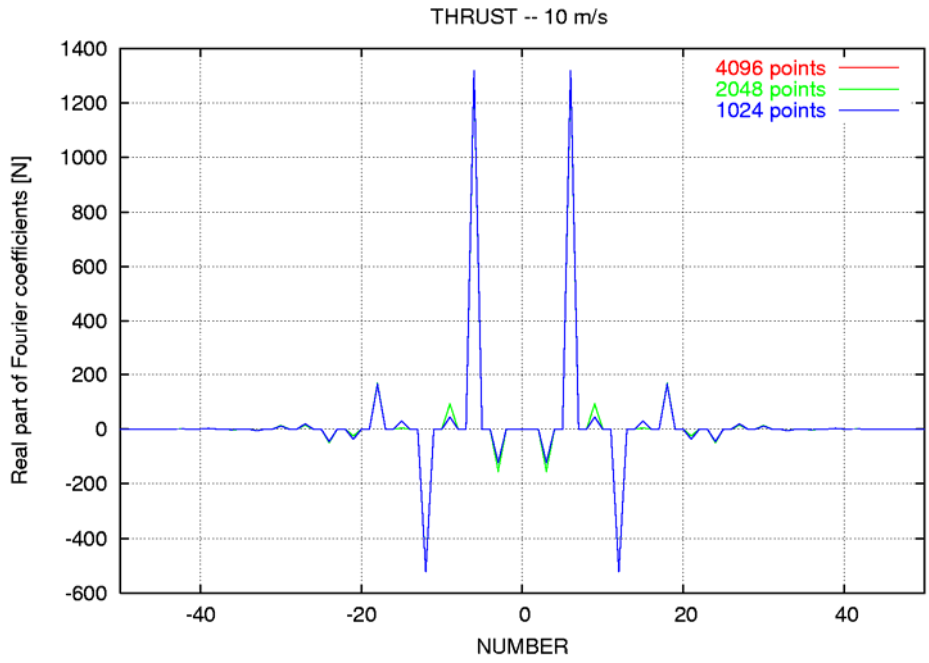

Figure 24 *Further test of the influence of time resolution.*

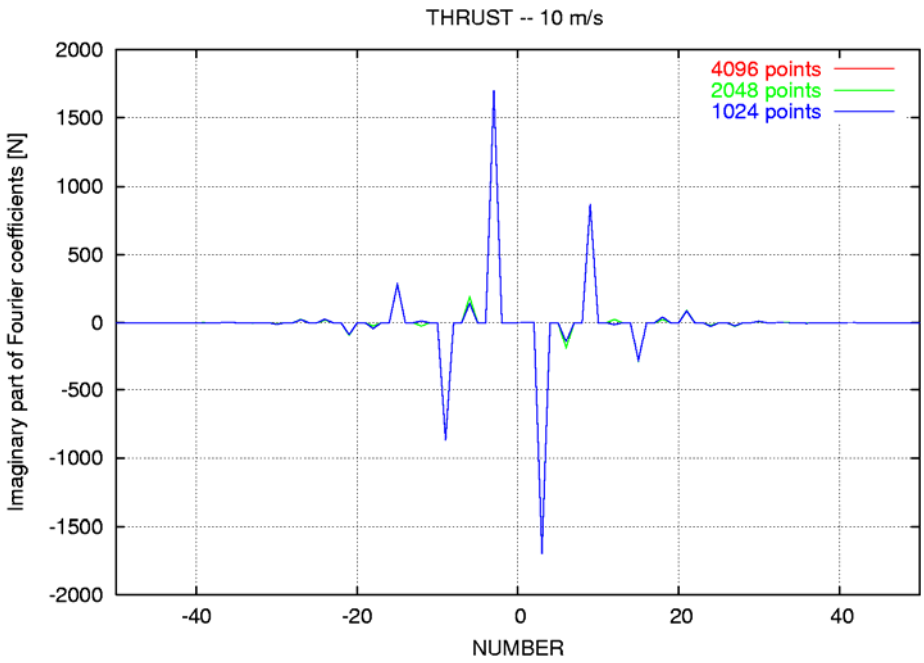

Figure 25 *Further test of the influence of time resolution.*

5 Appendix 2 – AIAA paper

45th AIAA Aerospace Sciences Meeting and Exhibit
8 - 11 January 2007, Reno, Nevada

AIAA 2007-623

Simulation of Low frequency Noise from a Downwind Wind Turbine Rotor

Helge Aa. Madsen[1], Jeppe Johansen, Niels N. Sørensen, Gunnar C. Larsen and Morten H. Hansen
Wind Energy Department, Risø National Laboratory, DK 4000 Roskilde, Denmark

Niels N. Sørensen
Department of Civil Engineering, Alborg University Wind Energy Department, Denmark and Wind Energy Department, Risø National Laboratory, DK-4000, Roskilde, Denmark

One of the major drawbacks of a wind turbine with a downwind rotor is the generation of considerable low frequency noise (so-called thumping noise) which can cause annoyance of people at a considerable distance. This was experienced on a number of full-scale turbines in e.g. US and Sweden in the period from around 1980 to 1990. One of the common characteristics of this low frequency noise, emerging from analysis of the phenomenon, was that the sound pressure level is strongly varying in time. We have investigated this phenomenon using a model package by which the low frequency noise of a downwind rotor can be simulated. In order to investigate the importance of wake unsteadiness, time true CFD computations of the flow past a 4 m diameter cylinder were performed at 8 m/s, and the wake characteristics were subsequently read into the aeroelastic code HAWC, which finally gives output to the aero acoustic model. The results for a 5 MW two-bladed turbine with a downwind rotor showed an increase in the sound pressure level of 5-20 dB due to the unsteadiness in the wake caused mainly by vortex shedding. However, in some periods the sound pressure level can increase additionally 0-10 dB when the blades directly pass through the discrete shed vortices behind the tower. The present numerical results strongly confirm the experiences with full scale turbines showing big variations of sound pressure level in time due to the wake unsteadiness, as well as a considerable increase in sound pressure level if the blade passing frequency is close to the Strouhal number controlling the vortex shedding from the tower.

Nomenclature

a_m^T = *Fourier coefficients of rotor thrust*
a_p^Q = *Fourier coefficients of rotor torque*
B = *number of blades*
c_0 = *speed of sound*
CD = *drag coefficient of tower*
D = *tower diameter*
f_b = *blade passing frequency*
f_r = *radial volume force*
f_v = *frequency of vortex shedding from the tower*
h = *tower height*
J = *standard Bessel function*
J_m = *momentum deficit*
K = *kinematic momentum*
P_n = *rms pressure variation of the n^{th} harmonic of the blade passage frequency*

[1] Research Specialist, Programme of Aeroelastic Design, Wind Energy Department, Risø National Laboratory, DK-4000 Roskilde, Denmark
helge.aagaard.madsen@risoe.dk +45 46775047

Q^s = *steady torque*
R = *tower radius*
r_m = *radius on blade, where thrust and torque is supposed to be concentrated*
SPL_n = *sound pressure level for the n^{th} harmonic*
s = *distance from listener to rotor*
T^s = *steady thrust*
U_0 = *free stream velocity*
u = *stream wise velocity component*
v = *lateral velocity component*
x = *stream wise coordinate*
y = *lateral coordinate*
η = *non-dimensional coordinate*
ϕ = *altitude angle from listener to rotor center*
γ = *azimuth angle from listener to rotor center*
ρ = *mass density*

I. Introduction

At the beginning of the development of modern wind turbines in the late seventies different rotor concepts were considered and investigated. Among them was the two-bladed teetered downwind rotor which has both advantages and drawbacks compared with the three-bladed upwind rotor. One of the advantages of a downwind rotor is that the blade flapwise deflection contributes positively to the blade tower clearance whereas this is opposite for an upstream rotor. Another advantage of the downwind two-bladed rotor is that the use of a teetering hinge can effectively reduce the bending moments transferred to the shaft when compared with a rotor with a stiff hub. Finally, a free yawing or high flexible yawing rotor concept is easier to obtain on a downwind rotor due to the restoring yaw moment from the rotor thrust.

However, a major drawback of the downwind rotor is a considerable generation of low frequency (thumping) noise typically in the range from 20 to 100 Hz which can cause annoyance of nearby residents. Low frequency noise was experienced on the MOD-1 2 MW turbine[1] and other downwind turbines in US[2] as well as on the 3 MW Maglarp turbine[3]. On all turbines the noise generation was linked to the blade passing the wake behind the tower which, for the Swedish turbine was a tubular tower, whereas the MOD-1 turbine had a lattice tower with four main poles.

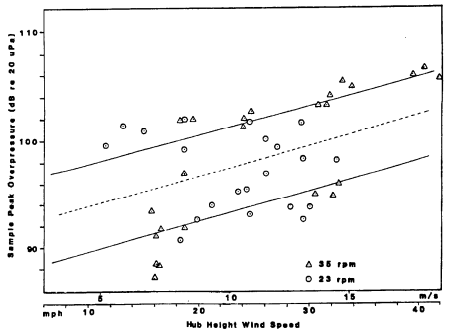

Figure 1. Considerable scatter in the measured sample peak impulse overpressure versus wind speed in the acoustic near-field of the MOD-1 turbine, from Ref. 1.

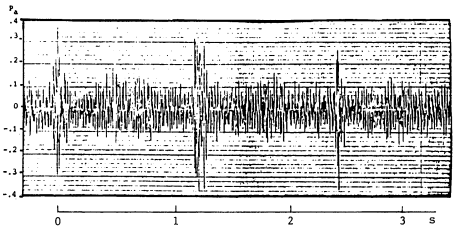

Figure 2. Time trace of sound pressure (2-2000 Hz) measured on ground level and 184 m downstream the tower of the Maglarp turbine showing considerable deviations from one blade passage to the next. From Ref. 2.

Another common characteristic of the measured noise was that it was varying strongly in time. This was seen as scatter with an amplitude of more than 10 dB in the overpressure versus wind speed measured at the MOD-1 turbine Fig. 1. Likewise in a time trace of measured sound pressure at the Maglarp turbine considerable differences are seen comparing the different blade passes Fig. 2. Kelly concludes about the acoustically generated pulses that " .. This process involves the turbine blade interaction with a transient level of wake instability and resulting intensity of velocity fluctuations and horizontal gradients in the wakes of the legs". Ljungren also mentions the importance of the dynamics in the wake and a good correlation between simulated and measured noise for the Maglarp turbine first was obtained when measured wake velocity profiles from the full scale turbine were used as input for the simulations.

A summary of the low frequency noise results from 8 different turbines in US are presented by Sheperd and Hubbard[4]. One of the concluding results is that the low frequency noise is only damped with 3 dB for doubling of distance in downwind direction. This means that even for off-shore application of down-wind rotors the low frequency noise could be a problem for residents along the cost lines.

In the present paper we will also focus on the importance of the unsteadiness of the wake behind the tower for the computed low frequency noise of a downwind MW rotor. The unsteady wake behind the tower is simulated with the 3D CFD code EllipSys3D. Time traces of the velocity components from this simulation are used in an aeroelastic simulation of a 5MW downwind turbine with a two-bladed teetering rotor, using the aeroelastic code HAWC. Finally, the Fourier coefficients of the time traces of simulated rotor thrust and torque are used as input in an acoustic model for prediction of the low frequency noise.

II. The model package

The computation of the low frequency noise is performed in a sequential manner involving a CFD model, an aeroelastic model including a wake deficit model and an acoustic model. Below these models are briefly described.

A. Navier-Stokes solver

The CFD code EllipSys3D is used for the tower computations. The code is developed by Michelsen[5,6] and Sørensen[7] and is a multiblock finite volume discretization of the incompressible Reynolds Averaged Navier-Stokes equations in general curvilinear coordinates. The code uses a collocated variable arrangement, and Rhie/Chow interpolation is used to avoid odd/even pressure decoupling. As the code solves the incompressible flow equations, no equation of state exists for the pressure and the PISO algorithm is used to enforce the pressure/velocity coupling. The EllipSys3D code is parallelized with MPI for executions on distributed memory machines, using a non-overlapping domain decomposition technique. Solution of the momentum equations is obtained using the third order accurate QUICK interpolation scheme for the convective terms. Unsteady computations are performed with a time step of 5.0×10^{-3}. The turbulent eddy viscosity is modeled using Detached-Eddy Simulation (DES) model according to Strelets[8].

The computational mesh is generated using the Risøs in-house grid generator HypGrid[9] The total number of computational cells is 4.7×10^{6}. On the entire surface of the tower geometry no-slip boundary conditions are used. On the outer boundary of the computational domain inflow velocity is assumed constant with zero shear and a low

turbulence intensity, while zero axial gradient is enforced at the outlet.

B. The aeoelastic model HAWC and the wake deficit model

The aeroelastic model HAWC[10] is based on a finite element formulation of the structural dynamics and a standard Blade Element Momentum modeling of the aerodynamics. Unsteady blade aerodynamics are modeled adopting the Leishman-Beddoes model[11].

In order to establish a queasy steady reference for the instantaneous CFD wake velocity profiles we developed a new model for the wake deficit behind a cylindrical tower based on the boundary layer solution for a jet flowing into a fluid at rest. In the new wake model (the JET wake model) the axial and lateral velocity components *u, v* develops according to the following equations:

$$u(x,\eta) = \frac{\sqrt{3}}{2}\sqrt{\frac{K\sigma}{x}}\left(1 - \tanh^2(\eta)\right) \tag{1}$$

$$v(x,\eta) = \frac{\sqrt{3}}{4}\sqrt{\frac{K}{x\sigma}}\left(2\eta\left(1 - \tanh^2(\eta)\right) - \tanh(\eta)\right) \tag{2}$$

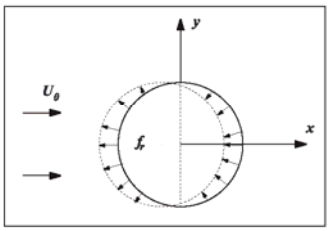

Figure 3. The source model for computation of the wake deficit behind the tower is comprised of radial directed volume forces distributed along a circle, a so-called actuator cylinder.

where $\eta = \sigma\frac{y}{x}$, x,y are non-dimensional (with respect to tower radius) Cartesian co-ordinates in the tower cross section, σ is an empirical constant equal to 7.67, and K is the kinematic momentum defined as $K = \frac{J_m}{\rho}$, where ρ is the mass density and J_m is the momentum deficit behind the tower defined by;

$$J_m = \rho\int_{-\infty}^{\infty}\left(u - U_0\right)^2 dy \tag{3}$$

where U_0 is the ambient undisturbed flow velocity.

A source model, with the volume forces distributed on a cylindrical surface **Fig. 3** (a so-called actuator cylinder) was used to obtain a correlation between the initial tower wake deficit and the drag coefficient of the tower.

For the source model the velocity components behind the tower can be derived as[12]:

For $|y| \geq 1$:

$$u = 1 + \frac{CD}{2\pi} \frac{x}{x^2 + y^2} \tag{4}$$

$$v = \frac{CD}{2\pi} \frac{y}{x^2 + y^2} \tag{5}$$

For $|y| \leq 1$:

$$u = 1 + \frac{CD}{2\pi} \left(\frac{x}{x^2 + y^2} - 4\sqrt{1 - y^2} \right) \tag{6}$$

$$v = \frac{CD}{2\pi} \frac{y}{x^2 + y^2} \tag{7}$$

x,y are dimensionless with respect to the tower radius R and the velocity components u,v dimensionless with respects to the free stream velocity . The tower drag is denoted CD .

Using the full developed velocity deficit according to (6) and inserting in (3) we finally obtain:

$$J_m = \frac{U_0^2 D}{2} \frac{\rho}{\pi} \left[\frac{1}{8} + \frac{16}{3\pi} \right] CD^2 \tag{8}$$

C. The acoustic model

The model used for calculating the sound pressure level from the Fourier coefficients of the unsteady thrust T and torque Q of the turbine, as simulated with the aeroelastic code, is originally due to Lowson[13], and the implementation of the model for computation of low frequency wind turbine noise is described by Viterna[14]. The latter formulation is followed here.

The RMS pressure variation of the n^{th} harmonic of the blade passage frequency is given by the following equations:

$$P_n = \frac{k_n \sqrt{2}}{4\pi s} \left\{ \sum_{p=1}^{\infty} \left[\begin{array}{l} e^{-im(\Phi - \pi/2)} J_{nB-p}\left(k_n r_m \sin\gamma\right) \cdot \left(a_p^T \cos\gamma - \dfrac{nB-p}{k_n r_m} a_p^Q \right) + \\ e^{im(\Phi - \pi/2)} J_{nB+p}\left(k_n r_m \sin\gamma\right) \cdot \left(a_{-p}^T \cos\gamma - \dfrac{nB+p}{k_n r_m} a_{-p}^Q \right) \end{array} \right] \right.$$

$$\left. + J_{nB}\left(k_n r_m \sin\gamma\right) \left(T^s \cos\gamma - \frac{nB}{k_n r_m} Q_s \right) \right\} \tag{9}$$

where $k_n = \frac{nB\Omega}{c_0}$

a_m^T, a_p^Q are Fourier coefficients of rotor torque and thrust, respectively.

B	number of blades
s	distance to rotor in [m]
γ, Φ	azimuth- og altitude angle, respectively, as taken from the point of observation to the rotor center, cf. Figure 4
r_m	radius on blade, where thrust and torque is supposed to be concentrated
J	standard Bessel function
c_0	speed of sound
T^s, Q^s	steady thrust and steady torque, respectively.

Finally, the sound pressure level SPL_n for each harmonic is computed as:

$$SPL_n = 10\log_{10}\left(\frac{P_n^2}{P_{ref}^2}\right) where \quad P_{ref} = 2\cdot 10^{-5}\,\text{Pa} \tag{10}$$

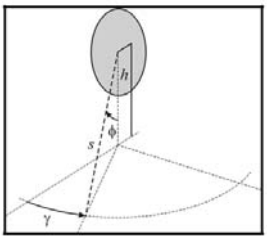

Figure 4. Definition of azimuth and altitude angles used in the acoustic model.

D. The model turbine

A 5MW two-bladed turbine with a 126 m diameter rotor and a tower height of 110 m was used for the present modeling of low frequency noise. The model is derived from a similar 3 bladed upwind model turbine designed by NREL[15] for used in the IEA Annex XXIII. To convert this three-bladed model to a two-bladed turbine we changed the planform simply by scaling the chord distribution with a factor 1.5 which then gives the same blade solidity for the two-bladed rotor. We used the same rotational speed as on the original three-bladed turbine which is 0.964 rad/s at a wind speed of 8 m/s which is the only wind speed that results will be presented for. On the original three-bladed turbine the tower diameter varies from 6 m at the bottom to 3.87 m at the top. This was changed to a constant tower diameter of 5 m on the two-bladed model. We did this in order to simplify interpretation of the results and for the same reason we also set the rotor coning and tilt to zero so that the blade has a constant distance to the tower. Finally, a teetering hub was introduced with a small teeter stiffness and damping. It should also be pointed out that all the aeroelastic simulations were run on a stiff model in order not to have major disturbances from structural dynamics on the noise characteristics.

III Results

E. CFD results for the flow past the cylinder

At the start of the present work a mesh for a 4 m diameter cylinder with a length of 16 m was already available, and so we used this although the tower on the turbine as mentioned above has a diameter of 5 m. The iso-vorticity surface for the simulated unsteady flow behind the cylinder shows clearly that vortex shedding occurs at a distance of about 1.5-2.0 D downstream of the tower center (the tower center will be used throughout the paper as reference for downstream distance) as seen in **Fig. 5**. This is also seen in the axial velocity contour plots at downstream distances of 1D, 2D, 3D and 4D in **Fig. 6.** At a distance of 1D the structures in the axial contour plot are relatively small when compared with e.g. the contours at a 2D distance indicating that the vortex shedding has not build up at the 1D distance. It is also seen that a considerable variation of the axial velocity contours in the length direction of the cylinder is present.

F. Results of aeroelastic simulations

The unsteady velocities from the CFD wake were read into the aeroelastic model and used as the free-stream velocity for the blades passing the wake at a specific downstream distance. A considerable simplification was introduced by neglecting the variation of velocities as function of position along the cylinder. This means that only the velocities at one plane (the plane perpendicular to the cylinder at the mid length of the cylinder) were used in the aeroelastic model and the velocities were then assumed coherent along the total blade length. The assumption might seem worse that it really is because the important part of the blade for noise generation is only the outer part towards the blade tip where we have the highest relative flow velocity to the blade. This means that the assumption of a coherent vortex shedding only has to be good on a minor part of the length of the cylinder corresponding in length to the outboard part of the blade. Another aspect is also the interaction of the blade with the flow around the tower which could make the vortex shedding from the tower more coherent along the tower.

We will first present computations for a downwind distance of three times the tower diameter (3.0D). This is probably at the high end of what is the necessary blade/tower clearance in order to avoid that the blade hits the tower but this depends strongly on the actual rotor design (max. teeter angle and blade stiffness). It seems that the distance was around 2.3D for the Maglarp turbine.

The instantaneous velocity profiles seen by the blade passing through the wake deficit shown in **Fig. 7** and **Fig. 8** show a considerable variation from one rev. to the next indicating that the blades are passing through a highly unsteady flow field. The wake deficits data from the CFD simulations had a length of 160 sec and for this period the instantaneous velocity profiles were binned as function of the lateral distance y from the tower center **Fig. 8**. It is seen that a good correlation was found between the average CFD wake deficit and the deficit computed with the JET wake model run with a drag coefficient CD for the tower of 0.6 which is a realistic value for a cylinder at a Reynolds number of around 3 mill as shown by Roshko[16]. However, the JET wake model does not show the small over speed of the velocity to slightly above the free stream velocity outside the wake region as is present in the CFD wake results.

The computed aerodynamic rotor thrust and rotor torque reflects directly the considerable unsteady wake deficit flow by strongly varying peaks when the blades passes the wake deficit, **Fig. 9** and **Fig. 10**. For both the rotor thrust and the rotor torque it is seen that also positive peaks can occur which are caused by a speed up of velocities in the wakes. For comparison is shown the response using the JET wake model which of course gives a constant variation in rotor thrust and torque.

Details of the angle of attack variations and the lift coefficient variations are shown in **Fig. 11**. and **Fig. 12** and the influence of the teeter motion is seen in the angle of attack response as a small deficit in angle of attack when the blade opposite to the present blade is passing through the wake deficit. The strong variation in CL over a very short interval indicates the need for modeling the unsteady blade section aerodynamics as is done with the Leishman Beddoes model in the present case.

G. Results of aero acoustic simulations and discussions

The Fourier coefficients of rotor thrust and torque is the input to the acoustic model from the aeroelastic model. For the Fourier analysis we used 22 segments each with a length of 1024 corresponding to one rev. Sound pressure levels (SPL) for a downstream distance of 3D for blade passage are shown in **Fig. 13**. The SPL for the unsteady wake deficit computed by CFD is seen to be typically 20 dB above the SPL computed on basis of the steady wake deficit from the JET wake model. We also computed the SPL on basis of a short time interval of the aeroelastic

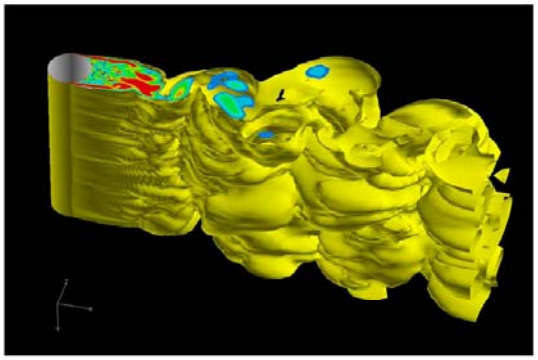

Figure 5. Iso-vorticity surface of the flow around a circular cylinder with a diameter D of 4 m, a length l equal to 16 m and at a wind speed of 8 m/s. In the top of the figure a contour plot of the vorticity is shown to illustrate the complexity of the flow structure right behind the cylinder.

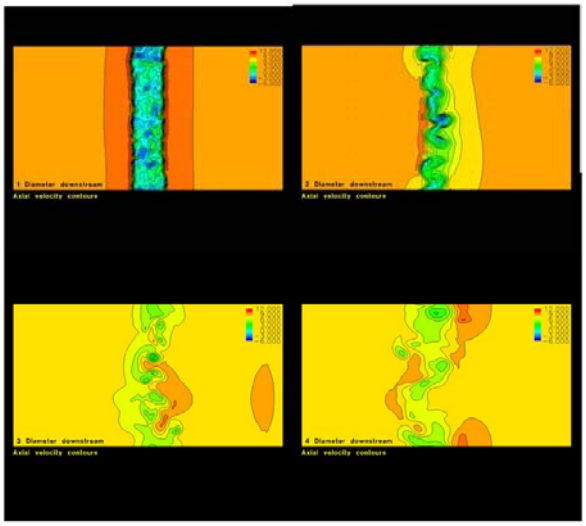

Figure 6. Axial velocity contours behind the tower at 4 distances: at 1D, 2D 3D and 4D.

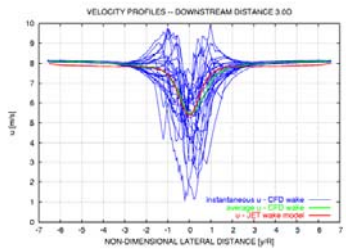

Figure 7. Instantaneous velocity profiles using CFD wake data compared with the steady state velocity profile from the JET wake model

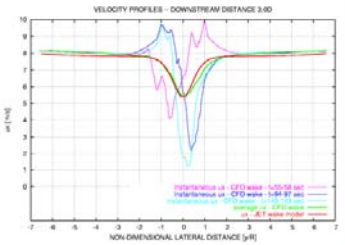

Figure 8. Details from Figure 7.

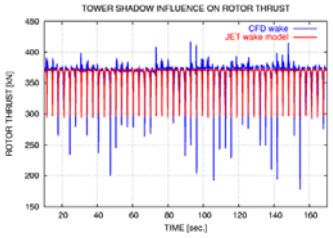

Figure 9. Rotor aerodynamic thrust using the instantaneous CFD wake data thrust and the steady JET wake deficit

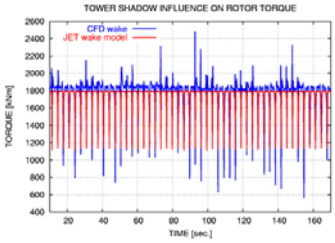

Figure 10. Rotor aerodynamic torque using the instantaneous CFD wake data and the steady JET wake deficit, respectively.

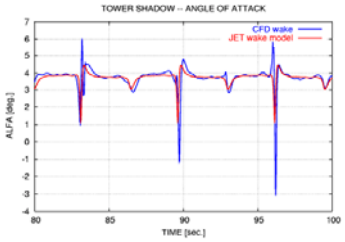

Figure 11. Details of angle of attack variations.

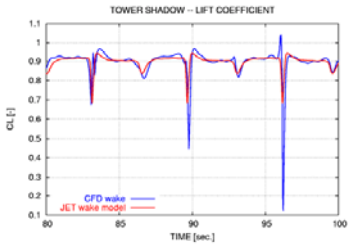

Figure 12. Details of lift variations.

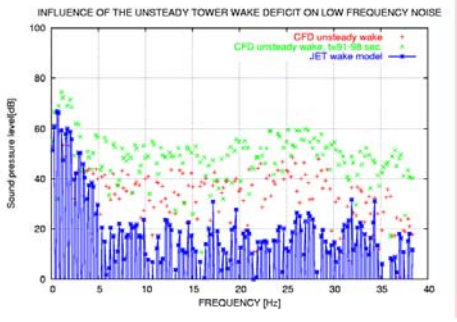

Figure 13. Computed sound pressure level at a distance of 200 m downstream the rotor showing the strong influence of the unsteady wake deficit flow on the low frequency noise.

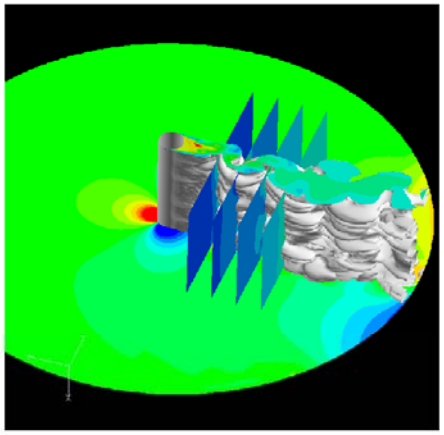

Figure 14. The influence on the low frequency noise from the downstream position of the rotor was analysed by extracting CFD wake data from 4 downstream positions, 2D 3D 4D and 5D.

simulation from t = 91-98 sec. where there were strong peaks in the time traces of thrust and torque as seen in **Fig. 9** and **Fig. 10**. For this case the SPL is seen to increase additional typical 10 dB.

We then investigated two extreme rotor/tower separations of 2D and 5D, respectively. The distance 2D corresponds to the plane closest to the tower in **Fig. 14** and it can be seen that it is just around the position where the vortex shedding process has fully developed. At 5D the vortex structures from vortex shedding are still present. The instantaneous velocity profiles shown in **Fig. 15** indicate that the unsteadiness in the flow has decreased considerably at a distance of 5D. Comparing the JET wake model with the average CFD wake deficit a good correlation is found at 5D whereas it seems that the JET model predicts the deficit too small at the 2D distance.

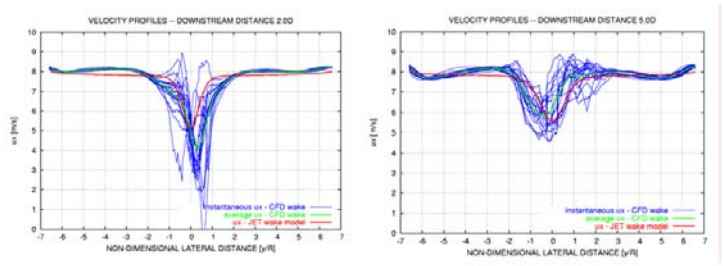

Figure 15. Velocity profiles at a downstream position of 2D and 5D, respectively.

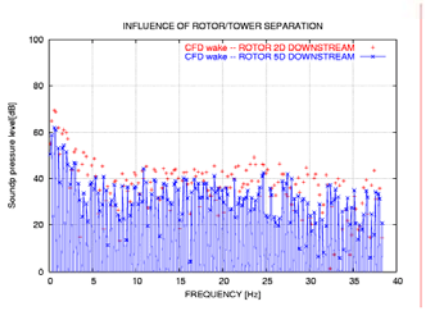

Figure 16. Comparison of predicted low frequency noise for two downwind rotor positions of 2D and 5D, respectively.

When comparing the predicted low frequency noise at the two positions as shown in **Fig.16** it is seen that the noise level has decreased at the 5D distance with around 5-10 dB but still remains at a level considerably higher than for the steady deficit at a distance of 3D shown in **Fig. 13.**

IV Conclusions

It has been demonstrated by simulations that the unsteadiness in the wake behind the tower plays a very important role for the level of the low frequency noise and that a realistic SPL cannot be computed using a steady, average wake deficit. The simulations have also shown that big variations between the pressure levels from one rev. to the next can occur, exactly as has been seen in full scale observations. The highest variations in thrust and torque are caused by the blade passing through the big vortices shed from the tower. There is thus the risk that the blade passing frequency f_b can coincide with the frequency of the vortex shedding f_v from the tower which is determined from the Strouhal number for the tower. According to Roshko the Strouhal number is in the range from 0.3-0.5 for a tower at a Reynolds number of 3 mill. and thus f_v will be in the range from 0.5-0.8 Hz at 8 m/s. f_b is 0.32 Hz at the present rotational speed and this means that 2 times f_b could coincide with f_v. These estimates on frequencies just illustrate that periods could occur with extraordinary high levels of low frequency noise due to the blades passing through vortices shed from the tower.

Design considerations should thus be taken to avoid or reduce the vortex shedding behind the tower and a great number of design proposals exist[17] as e.g. the well known screw formed plates on the tower or perforated shrouds. This has the draw back of increasing the drag of the tower and thus increasing the deficit but it seems that a stronger, steady deficit is better than a weaker but highly unsteady deficit.

IV References

[1]Kelly, N.D. "Acoustic Noise generation by the DOE/NASA MOD-1 Wind Turbine". Proceedings of Workshop "Wind Turbine Dynamics" held at Cleveland State University, Cleveland, Ohio, February 24-26, 1981. pp. 375-387.

[2] Hubbard, H. H. and Shepherd, K. P., "Aeroacoustics of large wind turbines," Journal of Acoustical Society of America **89** (6) June 1991, pp. 2495-2508

[3] Ljungren, S. "A Preliminary Assessment of Environmental Noise from large WECS, based on Experiences from Swedish Prototypes". Report FFA TN 1984-48.

[4] Shepherd, K.P. and Hubbard, H.H. "Physical Characteristics and Perception of Low Frequency Noise from Wind Turbine". Noise Control Engineering Journal, Volume 36 Number 1, January – February 1991.

[5] Michelsen JA "Basis3D - a Platform for Development of Multiblock PDE Solvers.", Technical Report AFM 92-05, Technical University of Denmark, 1992.

[6] Michelsen JA "Block structured Multigrid solution of 2D and 3D elliptic PDE's." Technical Report AFM 94-06, Technical University of Denmark, 1994.

[7] Sørensen NN "General Purpose Flow Solver Applied to Flow over Hills." Risø-R-827-(EN), Risø National Laboratory, Roskilde, Denmark, June 1995.

[8] Strelets M "Detached Eddy Simulation of Massively Separated Flows", AIAA 2001-0879, 2001.

[9] Sørensen N.N. "HypGrid2D a 2-D mesh generator", Risø-R-1035(EN), Risø National Laboratory, Roskilde, Denmark, 1998.

[10] Petersen, J.T. "The Aeroelastic Code HAWC – Model and Comparisons". In Proc. of the 28th IEA Expert Meeting. ´State of the Art Aeroelastic Codes´. Lyngby, Denmark 1996.

[11] Leishman, J.G. and beddoes, T.S. "A Generalised Model for Unsteady Airfoil Behaviour and Dynamic Stall Using the Indicial Method". Presented at the 42nd Annual Forum of the American Helicopter Society, Washington D.C., June 1986.

[12] Madsen, H.A., "The Actuator Cylinder – A Flow Model for Vertical Axis Wind Turbines". Ph.D. thesis report, Alborg University Centre, Aalborg, Denmark, January 1982.

[13] Lowson, M.V. "Theoretical Analysis of Compressor Noise Evaluation". J. Acoust. Soc. Am. , 47, 1 (part 2), pp 371-385, 1970.

[14] Viterna, L.A. "Method for Predicting Impulsive Noise Generated by Wind Turbine Rotors". Presented at Second DOE/NASA Wind Turbine Dyn. Workshop, Cleveland, 1981.

[15] Jonkman, J., IEA Annex XXIII document on NREL´s baseline wind turbine aeroelastic model. NREL/NWTC, August 11, 2005.

[16] Roshko, A. "Experiments on the flow past a circular cylinder at very high Reynolds number". Journal of Fluid Mechanics 10, pp. 345.

[17] Sumer, .M. and Fredsøe, J. "Hydrodynamics around Cylindrical Structures". Advanced Series on Ocean Engineering – Volume 12, World Scientific Publishing 1997. pp.411.

References

[1] Kelly, N.D. “Acoustic Noise generation by the DOE/NASA MOD-1 Wind Turbine”. Proceedings of Workshop “Wind Turbine Dynamics” held at Cleveland State University, Cleveland, Ohio, February 24-26, 1981. pp. 375-387.

[2] Hubbard, H. H. and Shepherd, K. P., “Aeroacoustics of large wind turbines,” Journal of Acoustical Society of America 89 (6) June 1991, pp. 2495-2508.

[3] Ljungren, S. “A Preliminary Assessment of Environmental Noise from large WECS, based on Experiences from Swedish Prototypes”. Report FFA TN 1984-48.

[4] Wagner, S., Bareiss, R., Guidatti, G. “Wind Turbine Noise”. Springer –Verlag Berlin Heidelberg 1996. European Commission (DGXII), EUR 16823.

[5] Shepherd, K.P. and Hubbard, H.H. “Physical Characteristics and Perception of Low Frequency Noise from Wind Turbines”. Noise Control Engineering Journal, Volume 36 Number 1, January – February 1991.

[6] Viterna, L.A. ”Method for Predicting Impulsive Noise Generated by Wind Turbine Rotors”. Presented at Second DOE/NASA Wind Turbine Dyn. Workshop, Cleveland, 1981.

[7] Madsen, H.A., Johansen, J., Sørensen, N.N., Larsen, G.C. and Hansen, M.H. “Simulation of Low frequency Noise from a Dowwind Wind Turbine Rotor. Paper AIAA 2007-623 presented at 45th AIAA Aerospace Sciences Meeting and Exhibit, 8-11 January 2007, Reno, Nevada, US.

[8] Lowson, M.V. ”Theoretical Analysis of Compressor Noise Evaluation”. J. Acoust. Soc. Am. , 47, 1 (part 2), pp 371-385, 1970.